

An efficient and accurate numerical method for the higher-order Boussinesq equation

Goksu Topkarcı^a, Handan Borluk^{b,*}, Gulcin M. Muslu^a

^a*Istanbul Technical University, Department of Mathematics, Maslak 34469, Istanbul, Turkey.*

^b*Istanbul Kemerburgaz University, Department of Basic Sciences, Bagcilar 34217, Istanbul, Turkey.*

Abstract

In the present paper, we are concerned with the higher-order Boussinesq (HBq) equation involving the parameter η_2 . We first derive the solitary wave solution and then we propose a Fourier pseudo-spectral scheme for the HBq equation. We prove the convergence of the semi-discrete scheme in the appropriate energy space. We study numerically behaviour of solutions to the HBq equation in the limit $\eta_2 \rightarrow 0$. Propagation and head-on collision of solitary waves are simulated numerically over long time intervals for various power type nonlinearities. Special attention is paid to the blow-up solutions of the higher-order Boussinesq equation.

Keywords: The higher-order Boussinesq equation, Fourier pseudo-spectral method, Solitary waves, Head-on collision of solitary waves, Blow-up
2010 MSC: 65M70, 35C07

1. Introduction

In the present paper, we will consider the higher-order Boussinesq (HBq) equation with the following initial conditions

$$u_{tt} = u_{xx} + \eta_1 u_{xxtt} - \eta_2 u_{xxxxtt} + (f(u))_{xx} \quad (1.1)$$

$$u(x, 0) = \phi(x), \quad u_t(x, 0) = \psi(x). \quad (1.2)$$

*Corresponding author

Email address: handan.borluk@kemerburgaz.edu.tr (Handan Borluk)

where $f(u) = u^p$, $p > 1$. Here η_1 and η_2 are real positive constants. The independent variables x and t denote spatial coordinate and time, respectively. The HBq equation was first derived by Rosenau [1] for the continuum limit of a dense chain of particles with elastic couplings. The HBq equation has been rederived to model the propagation of longitudinal waves in an infinite elastic medium with nonlinear and nonlocal properties by Duruk et. al. in [2]. HBq equation involving the linear term u_{xxxx} has been derived by Schneider & Wayne to model water waves with surface tension [3]. The HBq equation is also one of the class of nonlocal equation studied in [4] with the specific choice of the kernel $\beta(x)$ with Fourier transform is

$$\widehat{\beta}(\xi) = \frac{1}{1 + \eta_1 \xi^2 + \eta_2 \xi^4}.$$

When the parameter $\eta_2 = 0$, the HBq equation reduces to well-known generalized improved Boussinesq (IBq) equation

$$u_{tt} = u_{xx} + u_{xxtt} + (f(u))_{xx}.$$

The generalized IBq equation has been widely studied over the last couple of decades both numerically and analytically. The global existence of the Cauchy problem for the generalized IBq equation has been first proved by Chen & Wang in [5]. There are lots of numerical studies by using the finite differences, finite elements and spectral methods (see [6] and references in) to solve generalized IBq equation.

The local and global well-posedness of the Cauchy problem for the HBq equation in the Sobolev space H^s with any $s > 1/2$ and the regularity result has been proved by Duruk et. al. in [2]. As far as we know, there is no numerical study for HBq equation in the literature up to now. Our study is in response to the very natural questions: How the higher-order dispersive term and the various power type nonlinear terms affect the numerical solutions? Do numerical solutions of the HBq equation converge to solutions of the generalized IBq equation as $\eta_2 \rightarrow 0$?

In this study, to solve the HBq equations with various power type nonlinear terms, we use a Fourier pseudo-spectral method for the space discretization and a fourth-order Runge-Kutta scheme for time discretization. The paper is organized as follows: In Section 2, we review some properties of the HBq equation and then we derive the solitary wave solutions. In Section 3, we introduce the semi-discrete scheme and we then prove the convergence of

the semi-discrete scheme. In Section 4, we propose the fully-discrete Fourier pseudo-spectral scheme and show how to formulate it for the HBq equation. In Section 5, the numerical accuracy of the method is tested for various problems, like propagation of single solitary wave, head-on collision of two solitary waves and the blow-up solution.

2. Properties of the higher-order Boussinesq equation

In this section, we will review the conservation laws of the HBq equation and we will derive the solitary wave solution of the HBq equation by using ansatz method.

(a) *Conservation laws:* Three conserved quantities for the HBq equation are derived in [1, 4] in terms of U where $u = U_x$. The conserved quantities corresponding to mass, momentum and energy are respectively:

$$\mathcal{M}(t) = \int_{-\infty}^{\infty} U_t dx, \quad (2.1)$$

$$\mathcal{P}(t) = \int_{-\infty}^{\infty} U_x [U_t - \eta_1 U_{xxt} + \eta_2 U_{xxxxt}] dx \quad (2.2)$$

$$\mathcal{E}(t) = \int_{-\infty}^{\infty} [(U_t)^2 + 2F(U_x) + (U_x)^2 + \eta_1 (U_{xt})^2 + \eta_2 (U_{xxt})^2] dx \quad (2.3)$$

where $f(s) = F'(s)$.

(b) *Solitary wave solution:* We use the ansatz method which is the most effective direct method to construct the solitary wave solutions of the non-linear evolution equations. We look for the solutions of the form $u = u(\xi)$ where $\xi = x - ct - x_0$ under asymptotic boundary conditions. Substituting the solution $u = u(\xi)$ into eq. (1.1) and then integrating twice with respect to ξ , we have

$$(c^2 - 1)u - \eta_1 c^2 \frac{d^2 u}{d\xi^2} + \eta_2 c^2 \frac{d^4 u}{d\xi^4} = u^p \quad (2.4)$$

We now look for the solution of the form

$$u(\xi) = A \operatorname{sech}^\gamma(B\xi). \quad (2.5)$$

If we substitute the above ansatz into the eq. (2.4), the solitary wave solution

of the HBq equation are given in the form

$$u(x, t) = A \left\{ \operatorname{sech}^4 (B(x - ct - x_0)) \right\}^{\frac{1}{p-1}}, \quad (2.6)$$

$$A = \left[\frac{\eta_1^2 c^2 (p+1) (p+3) (3p+1)}{2\eta_2 (p^2 + 2p + 5)^2} \right]^{\frac{1}{p-1}}, \quad B = \left[\frac{\eta_1 (p-1)^2}{4\eta_2 (p^2 + 2p + 5)} \right]^{\frac{1}{2}}, \quad (2.7)$$

$$c^2 = \left\{ 1 - \left[\frac{4\eta_1^2 (p+1)^2}{\eta_2 (p^2 + 2p + 5)^2} \right] \right\}^{-1}. \quad (2.8)$$

where A is the amplitude and B is the inverse width of the solitary wave. Here c represents the the velocity of the solitary wave centered at x_0 with $c^2 > 1$.

3. The semi-discrete scheme

3.1. Notations and Preliminaries

Throughout this section, C denotes a generic constant. We use (\cdot, \cdot) and $\|\cdot\|$ to denote the inner product and the norm of $L^2(\Omega)$ defined by

$$(u, v) = \int_{\Omega} u(x)v(x)dx, \quad \|u\|^2 = (u, u) \quad (3.1)$$

for $\Omega = (-L, L)$, respectively. Let S_N be the space of trigonometric polynomials of degree $N/2$ defined as

$$S_N = \operatorname{span}\{e^{ik\pi x/L} \mid -N/2 \leq k \leq N/2 - 1\} \quad (3.2)$$

where N is a positive integer. $P_N : L^2(\Omega) \rightarrow S_N$ is an orthogonal projection operator

$$P_N u(x) = \sum_{k=-N/2}^{N/2-1} \hat{u}_k e^{ik\pi x/L} \quad (3.3)$$

such that for any $u \in L^2(\Omega)$

$$(u - P_N u, \varphi) = 0, \quad \forall \varphi \in S_N. \quad (3.4)$$

The projection operator P_N commutes with derivative in the distributional sense:

$$D_x^n P_N u = P_N D_x^n u \quad \text{and} \quad D_t^n P_N u = P_N D_t^n u. \quad (3.5)$$

Here D_x^n and D_t^n stand for the n th-order classical partial derivative with respect to x and t , respectively. $H_p^s(\Omega)$ denotes the periodic Sobolev space equipped with the norm

$$\|u\|_s^2 = \sum_{k=-\infty}^{\infty} (1 + |k|^{2s}) |\hat{u}_k|^2 \quad (3.6)$$

where $\hat{u}_k = \frac{1}{2L} \int_{\Omega} u(x) e^{ik\pi x/L} dx$. The Banach space $X_s = C^1([0, T]; H_p^s(\Omega))$ is the space of all continuous functions in $H_p^s(\Omega)$ whose distributional derivative is also in $H_p^s(\Omega)$, with norm $\|u\|_{X_s}^2 = \max_{t \in [0, T]} (\|u(t)\|_s^2 + \|u_t(t)\|_s^2)$. In order to prove the convergence of semi-discrete scheme, we need following lemmas.

Lemma 3.1. *[7, 8] For any real $0 \leq \mu \leq s$, there exists a constant C such that*

$$\|u - P_N u\|_{\mu} \leq C N^{\mu-s} \|u\|_s, \quad \forall u \in H_p^s(\Omega). \quad (3.7)$$

Lemma 3.2. *[9] Assume that $f \in C^k(\mathbb{R})$, $u, v \in H^s(\Omega) \cap L^\infty(\Omega)$ and $k = [s] + 1$, where $s \geq 0$. Then we have*

$$\|f(u) - f(v)\|_s \leq C(M) \|u - v\|_s \quad (3.8)$$

if $\|u\|_\infty \leq M, \|v\|_\infty \leq M, \|u\|_s \leq M$ and $\|v\|_s \leq M$, where $C(M)$ is a constant dependent on M and s .

Corollary 3.3. *Assume that $f \in C^3(\mathbb{R})$ and $u, v \in H^2(\Omega) \cap L^\infty(\Omega)$ then*

$$\|f(u) - f(v)\|_2 \leq C \|u - v\|_2 \quad (3.9)$$

where C is a constant dependent on $\|u\|_\infty, \|v\|_\infty$ and $\|u\|_2, \|v\|_2$.

3.2. Convergence of the semi-discrete scheme

The semi-discrete Fourier pseudo-spectral scheme for (1.1)-(1.2) is

$$u_{tt}^N = u_{xx}^N + \eta_1 u_{xxt}^N - \eta_2 u_{xxxxt}^N + P_N f(u^N)_{xx}, \quad (3.10)$$

$$u^N(x, 0) = P_N \phi(x), \quad u_t^N(x, 0) = P_N \psi(x) \quad (3.11)$$

where $u^N(x, t) \in S_N$ for $0 \leq t \leq T$. We now state our main result.

Theorem 3.4. *Let $s \geq 2$ and $u(x, t)$ be the solution of the periodic initial value problem (1.1)-(1.2) satisfying $u(x, t) \in C^1([0, T]; H_p^s(\Omega))$ for any $T > 0$ and $u^N(x, t)$ be the solution of the semi-discrete scheme (3.10)-(3.11). There exists a constant C , independent of N , such that*

$$\|u - u^N\|_{X_2} \leq C(T, \eta_1, \eta_2) N^{2-s} \|u\|_{X_s} \quad (3.12)$$

for the initial data $\phi, \psi \in H_p^s(\Omega)$.

Proof. Using the triangle inequality, it is possible to write

$$\|u - u^N\|_{X_2} \leq \|u - P_N u\|_{X_2} + \|P_N u - u^N\|_{X_2}. \quad (3.13)$$

Using Lemma 3.1, we have the following estimates

$$\|(u - P_N u)(t)\|_2 \leq C N^{2-s} \|u(t)\|_s$$

and

$$\|(u - P_N u)_t(t)\|_2 \leq C N^{2-s} \|u_t(t)\|_s$$

for $s \geq 2$. Thus, the estimation of the first term at the right-hand side of the inequality (3.13) becomes

$$\|u - P_N u\|_{X_2} \leq C N^{2-s} \|u\|_{X_s}. \quad (3.14)$$

Now, we need to estimate the second term $\|P_N u - u^N\|_{X_2}$ at the right-hand side of the inequality (3.13). Subtracting the equation (3.10) from (1.1) and taking the inner product with $\varphi \in S_N$ we have

$$((u - u^N)_{tt} - (u - u^N)_{xx} - \eta_1(u - u^N)_{xxtt} + \eta_2(u - u^N)_{xxxxtt} - (f(u) - P_N f(u^N))_{xx}, \varphi) = 0. \quad (3.15)$$

Since

$$((u - P_N u)_{tt}, \varphi) = ((u - P_N u)_{xx}, \varphi) = ((u - P_N u)_{xxtt}, \varphi) = ((u - P_N u)_{xxxxtt}, \varphi) = 0 \quad (3.16)$$

for all $\varphi \in S_N$, by (3.5), the equation (3.15) becomes

$$\begin{aligned} & (\{(P_N u - u^N)_{tt} - (P_N u - u^N)_{xx} - \eta_1(P_N u - u^N)_{xxtt} + \eta_2(P_N u - u^N)_{xxxxtt} \\ & \quad - (f(u) - f(u^N))_{xx}\}, \varphi) = 0 \end{aligned} \quad (3.17)$$

for all $\varphi \in S_N$. Setting $\varphi = (P_N u - u^N)_t$ in (3.17), using the integration by parts and the spatial periodicity, a simple calculation shows that

$$((P_N u - u^N)_{tt}, (P_N u - u^N)_t) = \frac{1}{2} \frac{d}{dt} \|(P_N u - u^N)_t(t)\|^2, \quad (3.18)$$

$$((P_N u - u^N)_{xx}, (P_N u - u^N)_t) = -\frac{1}{2} \frac{d}{dt} \|(P_N u - u^N)_x(t)\|^2, \quad (3.19)$$

$$((P_N u - u^N)_{xxtt}, (P_N u - u^N)_t) = -\frac{1}{2} \frac{d}{dt} \|(P_N u - u^N)_{xt}(t)\|^2, \quad (3.20)$$

$$((P_N u - u^N)_{xxxxtt}, (P_N u - u^N)_t) = \frac{1}{2} \frac{d}{dt} \|(P_N u - u^N)_{xxt}(t)\|^2. \quad (3.21)$$

Substituting (3.18)-(3.21) in (3.17), we have

$$\begin{aligned} \frac{1}{2} \frac{d}{dt} [\|(P_N u - u^N)_t(t)\|^2 + \|(P_N u - u^N)_x(t)\|^2 + \eta_1 \|(P_N u - u^N)_{xt}(t)\|^2 \\ + \eta_2 \|(P_N u - u^N)_{xxt}(t)\|^2] = ((f(u) - f(u^N))_{xx}, (P_N u - u^N)_t). \end{aligned} \quad (3.22)$$

In the following, we will estimate the right-hand side of the above equation.

Using the Cauchy-Schwarz inequality and the Corollary 3.3, we have

$$\begin{aligned} ((f(u) - f(u^N))_{xx}, (P_N u - u^N)_t) &\leq \|(f(u) - f(u^N))_{xx}\| \|(P_N u - u^N)_t(t)\| \\ &\leq \frac{1}{2} (\|f(u) - f(u^N)\|_2^2 + \|(P_N u - u^N)_t(t)\|^2) \\ &\leq C (\|(u - u^N)(t)\|_2^2 + \|(P_N u - u^N)_t(t)\|^2). \end{aligned} \quad (3.23)$$

Substituting (3.23) in (3.22) we have

$$\begin{aligned} \frac{1}{2} \frac{d}{dt} (\|(P_N u - u^N)_t(t)\|^2 + \|(P_N u - u^N)_x(t)\|^2 + \eta_1 \|(P_N u - u^N)_{xt}(t)\|^2 \\ + \eta_2 \|(P_N u - u^N)_{xxt}(t)\|^2) \\ \leq C (\|(u - u^N)(t)\|_2^2 + \|(P_N u - u^N)_t(t)\|^2) \\ \leq C (\|(u - P_N u)(t)\|_2^2 + \|(P_N u - u^N)(t)\|_2^2 + \|(P_N u - u^N)_t(t)\|^2) \end{aligned} \quad (3.24)$$

Adding the terms $(P_N u - u^N, (P_N u - u^N)_t)$ and $((P_N u - u^N)_{xx}, (P_N u - u^N)_{xxt})$ to both sides of the equation (3.24) becomes

$$\begin{aligned} \frac{1}{2} \min\{1, \eta_1, \eta_2\} \frac{d}{dt} [\|(P_N u - u^N)(t)\|_2^2 + \|(P_N u - u^N)_t(t)\|_2^2] \\ \leq C (\|(u - P_N u)(t)\|_2^2 + \|(P_N u - u^N)(t)\|_2^2 + \|(P_N u - u^N)_t(t)\|_2^2) \end{aligned}$$

Note that $\|(P_N u - u^N)(0)\|_2 = 0$ and $\|(P_N u - u^N)_t(0)\|_2 = 0$. The Gronwall Lemma and Lemma 3.1 imply that

$$\begin{aligned} \|(P_N u - u^N)(t)\|_2^2 + \|(P_N u - u^N)_t(t)\|_2^2 &\leq \int_0^t \|u(\tau) - P_N u(\tau)\|_2^2 e^{C(t-\tau)} d\tau \\ &\leq C(T, \eta_1, \eta_2) N^{4-2s} \int_0^t \|u(\tau)\|_s^2 d\tau \end{aligned} \quad (3.25)$$

for $s \geq 2$. Finally, we have

$$\|P_N u - u^N\|_{X_2} \leq C(T, \eta_1, \eta_2) N^{2-s} \|u\|_{X_s}. \quad (3.26)$$

Using (3.14) and (3.26) in (3.13), we complete the proof of Theorem 2.4. \square

4. The fully-discrete scheme

We solve the HBq equation by combining a Fourier pseudo-spectral method for the space component and a fourth-order Runge Kutta scheme (RK4) for time. If the spatial period $[-L, L]$ is, for convenience, normalized to $[0, 2\pi]$ using the transformation $X = \pi(x + L)/L$, the equation (3.10) becomes

$$u_{tt}^N - \left(\frac{\pi}{L}\right)^2 u_{XX}^N - \eta_1 \left(\frac{\pi}{L}\right)^2 u_{XXtt}^N + \eta_2 \left(\frac{\pi}{L}\right)^4 u_{XXXXtt}^N = \left(\frac{\pi}{L}\right)^2 (u^N)^p_{XX}. \quad (4.1)$$

The interval $[0, 2\pi]$ is divided into N equal subintervals with grid spacing $\Delta X = 2\pi/N$, where the integer N is even. The spatial grid points are given by $X_j = 2\pi j/N$, $j = 0, 1, 2, \dots, N$. The approximate solutions to $u^N(X_j, t)$ are denoted by $U_j(t)$. The discrete Fourier transform of the sequence $\{U_j\}$, i.e.

$$\tilde{U}_k = \mathcal{F}_k[U_j] = \frac{1}{N} \sum_{j=0}^{N-1} U_j \exp(-ikX_j), \quad -\frac{N}{2} \leq k \leq \frac{N}{2} - 1. \quad (4.2)$$

gives the corresponding Fourier coefficients. Likewise, $\{U_j\}$ can be recovered from the Fourier coefficients by the inversion formula for the discrete Fourier transform (4.2), as follows:

$$U_j = \mathcal{F}_j^{-1}[\tilde{U}_k] = \sum_{k=-\frac{N}{2}}^{\frac{N}{2}-1} \tilde{U}_k \exp(ikX_j), \quad j = 0, 1, 2, \dots, N-1. \quad (4.3)$$

Here \mathcal{F} denotes the discrete Fourier transform and \mathcal{F}^{-1} its inverse. These transforms are efficiently computed using a fast Fourier transform (FFT) algorithm.

Applying the discrete Fourier transform to the eq. (4.1) we get the second order ordinary differential equation which can be written in the following system

$$(\tilde{U}_k)_t = \tilde{V}_k \quad (4.4)$$

$$(\tilde{V}_k)_t = -\frac{(\pi k/L)^2}{1 + \eta_1(\pi k/L)^2 + \eta_2(\pi k/L)^4} [\tilde{U}_k + (\tilde{U}^p)_k]. \quad (4.5)$$

In order to handle the nonlinear term we use a pseudo-spectral approximation. That is, we use the formula $\mathcal{F}_k[(U_j)^p]$ to compute the k^{th} Fourier component of u^p . We use the fourth-order Runge-Kutta method to solve the resulting ODE system (4.4)-(4.5) in time. Finally, we find the approximate solution by using the inverse Fourier transform (4.3).

5. Validation of the fully-discrete scheme

The purpose of the present numerical experiments is to verify numerically (i) that the proposed Fourier pseudo-spectral scheme is highly accurate, (ii) that the scheme exhibits the fourth-order convergence in time and (iii) that the scheme has spectral accuracy in space. We will consider propagation of a single solitary wave, head-on collision of two solitary waves and blow-up of a solution. L_∞ -error norm is defined as

$$L_\infty\text{-error} = \max_i |u_i - U_i| \quad (5.1)$$

where u_i denotes the exact solution at $u(X_i, t)$. We use fast Fourier transform (FFT) routines in Matlab (i.e. fft and ifft) to calculate Fourier transform and the inverse Fourier transform.

5.1. Propagation of a Single Solitary Wave

We first study the single solitary wave solution of the HBq equation for quadratic nonlinearity. For $\eta_1 = \eta_2 = 1$ the initial conditions corresponding to the solitary wave solution (2.6) become as follows:

$$u(x, 0) = A \operatorname{sech}^4(B x), \quad (5.2)$$

$$v(x, 0) = 4 A B c \operatorname{sech}^4(B x) \tanh(B x). \quad (5.3)$$

For $\eta_1 = \eta_2 = 1$ the solution represents a solitary wave initially at $x_0 = 0$ moving to the right with the amplitude $A \approx 0.39$, speed $c \approx 1.13$ and $B \approx 0.14$. The problem is solved on the space interval $-100 \leq x \leq 100$ for times up to $T = 5$ where $\Delta x = 2L/N$ and $\Delta t = T/M$. We show the variation of L_∞ -errors with N for the HBq equation for various powers of nonlinearity, namely, $f(u) = u^p$ for $p = 2, 3, 4, 5$ in Figure 1. The value of M is chosen to satisfy $\nu = \Delta t / \Delta x = 2.56 \times 10^{-2}$. We observe that the L_∞ -errors decay as the number of grid points increases for various degrees of nonlinearity. Even in the case of the quintic nonlinearity, the L_∞ -errors are about 10^{-12} . To compare our numerical results we have not seen any numerical results for the HBq eq. in the literature. This experiment shows that the proposed method provides highly accurate numerical results even for the higher-order nonlinearities.

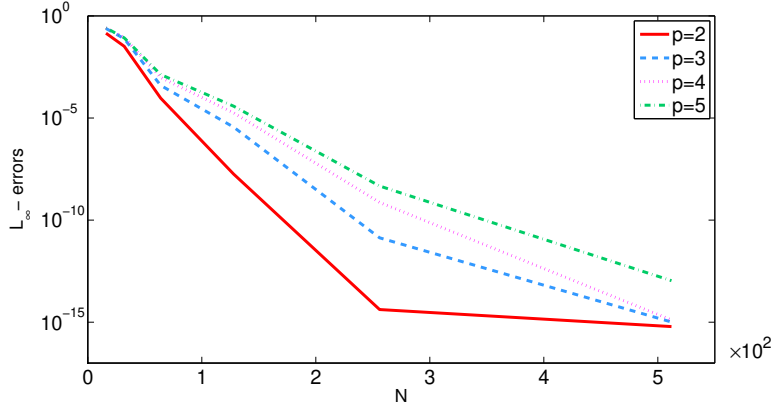


Figure 1: L_∞ -errors for the increasing values of N .

To validate whether the Fourier pseudo-spectral method exhibits the expected convergence rates in time we perform some numerical experiments for various values of M and a fixed value of N . In these experiments we take $N = 512$ to ensure that the error due to the spatial discretization is negligible. The convergence rates calculated from the L_∞ -errors for the terminating time $T = 5$ are shown in Table I. The computed convergence rates agree well with the fact that Fourier pseudo-spectral method exhibits the fourth-order convergence in time.

TABLE I

The convergence rate in time calculated from the L_∞ -errors in the case of single solitary wave ($A \approx 0.39$, $N = 512$).

M	L_∞ -error	Order
2	8.662E-3	-
5	2.530E-4	3.8561
10	1.614E-5	3.9704
50	2.623E-8	3.9903
100	1.637E-9	4.0021

To validate whether the Fourier pseudo-spectral method exhibits the expected convergence rate in space we perform some further numerical experiments for various values of N and a fixed value of M . In these experiments we take $M = 1000$ to minimize the temporal errors. We present the L_∞ -errors for the terminating time $T = 5$ together with the observed rates of convergence in Table II.

TABLE II

The convergence rates in space calculated from the L_∞ -errors in the case of the single solitary wave ($A \approx 0.39$, $M = 1000$).

N	L_∞ -error	Order
10	0.211E-1	-
50	1.747E-3	1.5480
100	4.431E-7	11.9450
150	6.500E-10	16.0916
200	3.884E-13	25.8017

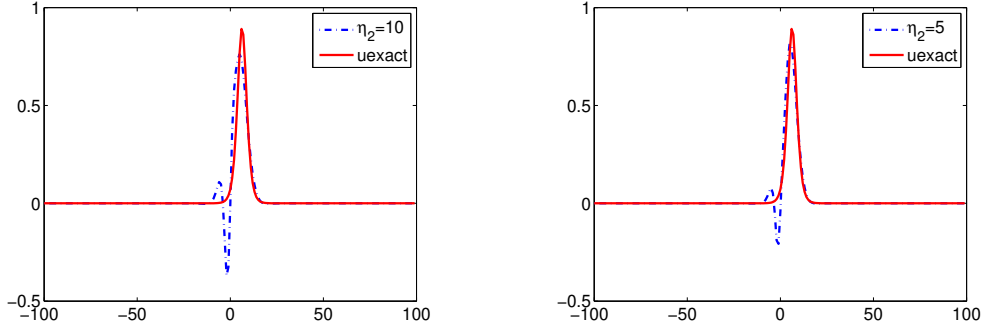
These results show that the numerical solution obtained using the Fourier pseudo-spectral scheme converges rapidly to the accurate solution in space, which is an indicative of exponential convergence. The question arises naturally how the solitary wave solutions of the HBq equation behaves when $\eta_2 \rightarrow 0$. For this aim, we perform some numerical tests for various values of

η_2 and the fixed value $\eta_1 = 1$ by using the initial condition

$$u(x, 0) = A \operatorname{sech}^2\left(\frac{1}{c}\sqrt{\frac{A}{6}} x\right), \quad (5.4)$$

$$v(x, 0) = 2 A \operatorname{sech}^2\left(\frac{1}{c}\sqrt{\frac{A}{6}} x\right) \tanh\left(\frac{1}{c}\sqrt{\frac{A}{6}} x\right) \quad (5.5)$$

where $A = 0.25$ and $c = \pm\sqrt{\frac{2A}{3}} + 1$. In Figure 2, the solid line shows the exact solution of the improved Boussinesq equation given in [6] and the dashed lines show the numerical solution of the HBq equation for the values of $\eta_2 = 10$, $\eta_2 = 5$, $\eta_2 = 1$ and $\eta_2 = 0.1$. The numerical tests show that the solitary wave solutions of the HBq equation converge to the solitary wave solution of the improved Boussinesq equation.



5.2. Head-on Collision of Two Solitary Waves

In this section, we consider the HBq equation with quadratic nonlinearity. In the second numerical experiment we study the head-on collision of two solitary waves with equal amplitudes. The initial conditions are given by

$$u(x, 0) = \sum_{i=1}^2 A \operatorname{sech}^4(B(x - x_0^i)),$$

$$v(x, 0) = 4 \sum_{i=1}^2 A B c_i \operatorname{sech}^4(B(x - x_0^i)) \tanh(B(x - x_0^i)).$$

We consider two solitary waves, one initially located at $x_0^1 = -40$ and moving to the right with amplitude A ($c_1 > 0$) and one initially located at $x_0^2 =$

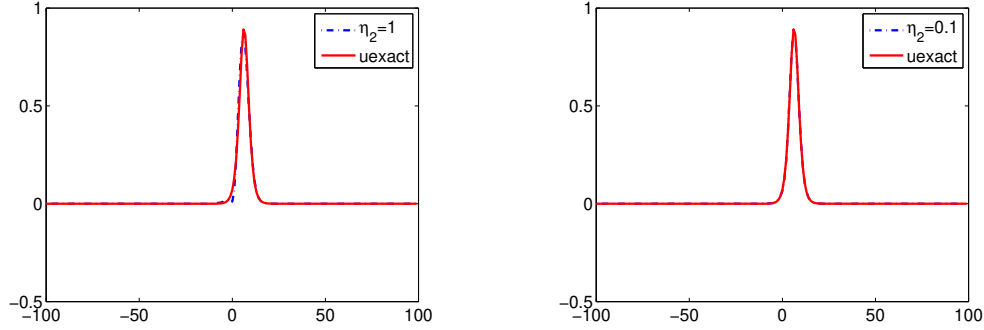


Figure 2: The numerical solution of the HBq eq. for $\eta_2 = 10$, $\eta_2 = 5$, $\eta_2 = 1$, $\eta_2 = 0.1$ and a fixed value $\eta_1 = 1$.

40 and moving to the left with amplitude A ($c_2 = -c_1$). The problem is solved again on the interval $-100 \leq x \leq 100$ for times up to $T = 72$ using the Fourier pseudo-spectral method. All experiments in this section are performed for $\Delta x = 0.4$ and $\Delta t = 10^{-2}$. We first illustrate the head-on collision of two solitary waves with equal amplitudes $A \approx 0.39$ and $A \approx 1.08$ in Figure 3.

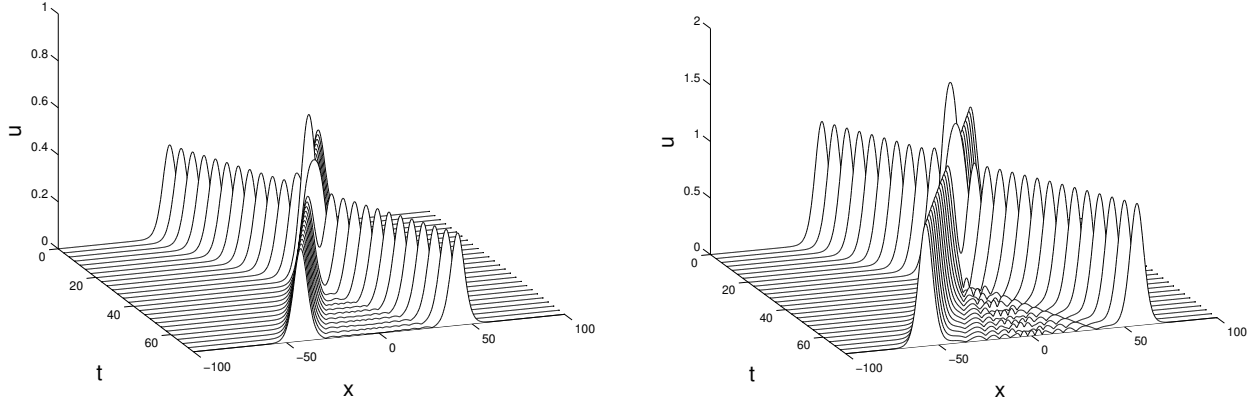


Figure 3: Surface plot of the head-on collision of two solitary waves with equal amplitudes. $A \approx 0.39$ (left panel) and $A \approx 1.08$ (right panel).

As the HBq equation cannot be solved by the inverse scattering method, so the interaction of solitary waves are inelastic. Although secondary waves

exist in all nonlinear interactions, they become more visible as we increase the amplitudes of the interacting waves. Since an analytical solution is not

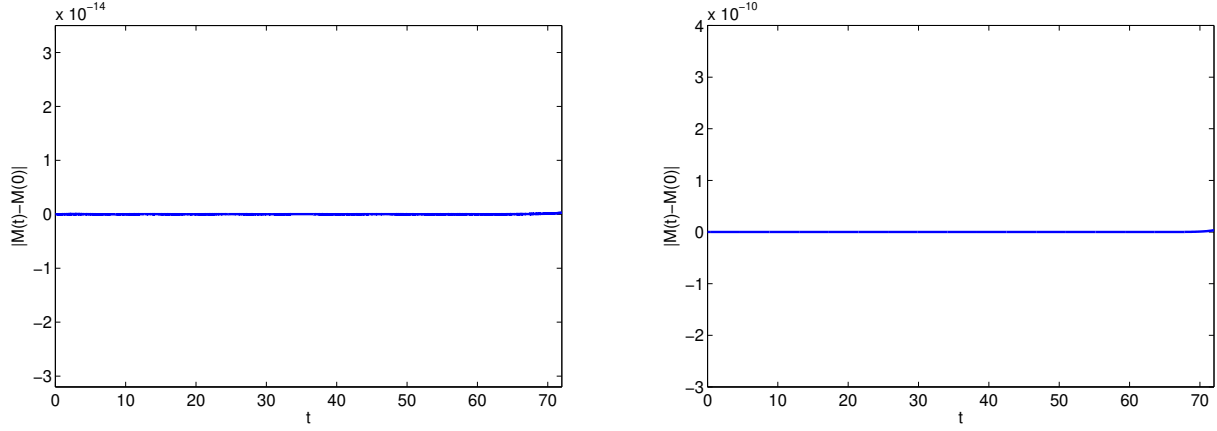


Figure 4: Evolution of the change in the conserved quantity \mathcal{M} (mass) for $A \approx 0.39$ (left panel) and $A \approx 1.08$ (right panel).

available for the collision of two solitary waves, we cannot present the L_∞ -errors for this experiment. But, as a numerical check of the proposed Fourier pseudo-spectral scheme, we present the evolution of the change in the conserved quantity \mathcal{M} (mass) in Figure 4 for the amplitudes $A \approx 0.39$ and $A \approx 1.08$. As can be seen from the figure, the conserved quantity (mass) remains constant in time and this behavior provides a valuable check on the numerical results.

5.3. Blow-up Solution

In the last section, we test the ability of the Fourier pseudo-spectral method to detect blow-up solutions of the HBq equation by comparing the analytical blow-up result given in [4]. Throughout this section, we set the parameters $\eta_1 = \eta_2 = 1$ in (1.1). The HBq equation is one of the class of nonlocal equation, we refer to Theorem 5.2 in [4] as the blow-up criteria. Applied to the HBq equation, this theorem can be restated as:

Theorem 5.1. *Suppose $\phi = \Phi_x, \psi = \Psi_x$ for some $\Phi, \Psi \in H^2(\Omega)$ and $F(\varphi) \in L^1(\Omega)$. If there are some $\mu > 0$ such that*

$$pf(p) \leq 2\mu p^2 + 2(1 + 2\mu)F(p) \text{ for all } p \in \mathbb{R}, \quad (5.6)$$

and $\mathcal{E}(0) < 0$, then the solution u of the Cauchy problem for HBq equation with the initial conditions $u(x, 0) = \phi(x)$, $u_t(x, 0) = \psi(x)$ blows up in finite time.

In the first experiment, we consider the quadratic nonlinearity. If we choose the initial conditions

$$\phi(x) = 4 \left(\frac{2x^2}{3} - 1 \right) e^{-\frac{x^2}{3}}, \quad \psi(x) = (x^2 - 1) e^{-\frac{x^2}{3}} \quad (5.7)$$

as in [10], then the conditions for the blow-up are satisfied for $\mu = \frac{1}{4}$. The problem is solved on the interval $-10 \leq x \leq 10$ for times up to $T = 4$. We present the variation of the L_∞ norm of the approximate solution obtained using the Fourier pseudo-spectral scheme for $N = 64$ and $M = 400$ in Figure 5. We point out that the initial amplitude is 4 in the initial condition given by eq. (5.7). However, the amplitude of the numerical solution increases as time increases and it becomes approximately 10^{94} near the numerical blow-up time. The numerical results strongly indicate that a blow-up is well underway by time $t = 3.8$. Therefore, there is a good agreement between the numerical and analytical results.

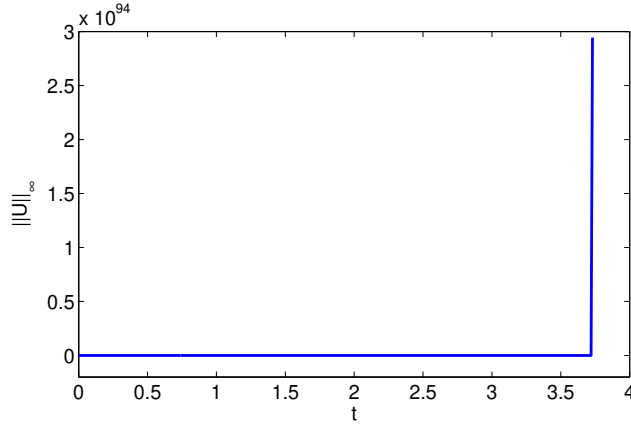


Figure 5: The variation of $\|U\|_\infty$ with time.

In the second numerical experiment, we consider the cubic nonlinearity. We choose the initial conditions as

$$\phi(x) = 13 \left(\frac{x^2}{2} - 1 \right) e^{-\frac{x^2}{4}}, \quad \psi(x) = (1 - x^2) e^{-\frac{x^2}{2}}. \quad (5.8)$$

where $\mathcal{E}(0) < 0$. In this case, the inequality (5.6) is satisfied for $\mu = \frac{1}{2}$. The problem is solved on the interval $-10 \leq x \leq 10$ for times up to $T = 0.4$. We present the variation of the L_∞ norm of the approximate solution for $N = 64$ and $M = 40$ in Figure 6. The amplitude of the numerical solution increases as time increases. The numerical results strongly indicate that a blow-up is well underway by time $t = 0.36$. Good agreement between the numerical and analytical results shows that the Fourier pseudo-spectral method does not miss the blow-up solutions.

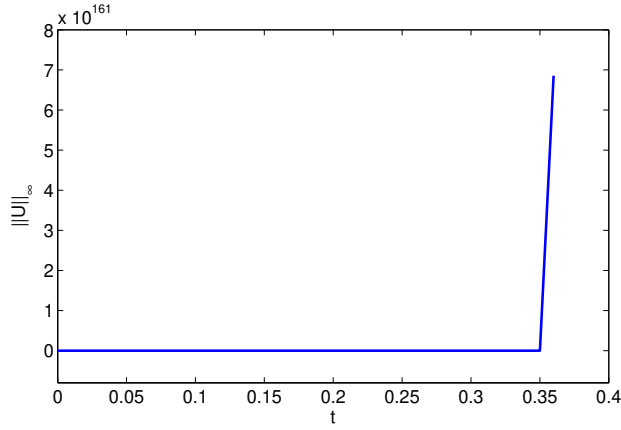


Figure 6: The variation of $\|U\|_\infty$ with time.

Acknowledgement: This work has been supported by the Scientific and Technological Research Council of Turkey (TUBITAK) under the project MFAG-113F114.

References

- [1] P. Rosenau, Dynamics of dense lattices, *Phys. Rev. B* 36 (1987) 5868–5876.
- [2] N. Duruk, A. Erkip, H. A. Erbay, A higher-order Boussinesq equation in locally non-linear theory of one-dimensional non-local elasticity, *IMA J. Appl. Math.* 74 (2009) 97–106.
- [3] G. Schneider, C. E. Wayne, Kawahara dynamics in dispersive media, *Physica D: Nonlinear Phenomena* 152 (2001) 384–394.
- [4] N. Duruk, H. A. Erbay, A. Erkip, Global existence and blow-up for a class of nonlocal nonlinear cauchy problems arising in elasticity, *Nonlinearity* 23 (2010) 107–118.
- [5] G. W. Chen, S. Wang, Existence and nonexistence of global solutions for the generalized IMBq equation, *Nonlinear Analysis: Theory Methods & Applications* 36 (1999) 961–980.
- [6] H. Borluk, G. M. Muslu, A Fourier pseudospectral method for a generalized improved Boussinesq equation, *Numerical Methods for Partial Differential Equations* DOI: 10.1002/num.21928.
- [7] C. Canuto, A. Quarteroni, Approximation results for orthogonal polynomials in sobolev spaces, *Mathematics of Computation* 38 (1982) 67–86.
- [8] A. Rashid, S. Akram, Convergence of fourier spectral method for resonant long-short nonlinear wave interaction, *Applications of Mathematics* 55 (2010) 337–350.
- [9] T. Runst, W. Sickel, Sobolev spaces of fractional order, Nemytskij operators, and nonlinear partial differential equations, Vol. 3, Walter de Gruyter, 1996.
- [10] A. Godefroy, Blow-up solutions of a generalized Boussinesq equation, *IMA J. Numer. Anal.* 60 (1998) 122–138.